PERGAMON

Solid State Communications 114 (2000) 441–445

solid state communications

www.elsevier.com/locate/ssc

Giant magneto-optical anisotropy in Fe/Au monoatomic multilayer

L. Uba[a,*], S. Uba[a], V.N. Antonov[a,b], A.N. Yaresko[c], A.Ya. Perlov[c], T. Ślęzak[d], J. Korecki[d]

[a]*Institute of Experimental Physics, University of Bialystok, Lipowa 41, PL-15-424 Bialystok, Poland*
[b]*Institute of Metal Physics, 36 Vernadskii str., 252142 Kiev, Ukraine*
[c]*Max-Planck-Institut for the Physics of Complex Systems, D-01187 Dresden, Germany*
[d]*Department of Solid State Physics, Faculty of Physics and Nuclear Techniques, University of Mining and Metallurgy, 30-059 Krakow, Poland*

Received 7 February 2000; received in revised form 14 February 2000; accepted 15 February 2000 by M. Grynberg

Abstract

A giant magneto-optical anisotropy (MOA) in a magnetic monoatomic Fe/Au multilayer structure is reported. The dependence of the off-diagonal part of the optical conductivity tensor on the angle between the magnetization and crystallographic axes is evidenced by measurements of both the polar and longitudinal Kerr effects. The microscopic origin of the MOA is elucidated on the basis of the first principles' band-structure calculations. A relationship of the MOA with the predicted strong anisotropy of Fe d orbital magnetic moment and the magnetocrystalline anisotropy is discussed. © 2000 Elsevier Science Ltd. All rights reserved.

Keywords: A. Magnetic films and multilayers; D. Optical properties; D. Electronic band structure; D. Spin–orbit effects

1. Introduction

Many important physical properties of crystals depend on the relative orientation of the magnetization and the crystallographic axes as the spin subsystem is coupled to the lattice by the spin–orbit (SO) interaction. The magnetocrystalline anisotropy (MCA), which is the energy that directs the magnetization along a certain crystallographic axis, is a ground state property of a crystal. The magneto-optical anisotropy (MOA), defined as the dependence of the off-diagonal part of the optical conductivity on the magnetization direction, arises as a result of electronic excitations and is due to the spin and orbital polarizations of initial and final states.

Whereas the MCA has been widely studied both experimentally [1] and theoretically [2–5], the investigations of the MOA are still elementary. Theoretical calculations were performed for Co, FePt, CoPt [6], CoPd [7], and CrO_2 [8]. Experimentally, the MO anisotropy was investigated in details only for Co [9–11]. In particular, Weller et al. [10] studied the orientation dependence of the magneto-optical (MO) properties measuring the MO Kerr effect in polar geometry (PKE) for two (0001) and $(11\bar{2}0)$ epitaxial hcp Co films. The maximal anisotropy of the Kerr rotation of ~20% was observed.

In recent years, artificial multi-layered structures (MLS) attract a lot of interest due to their unique physical properties. They exhibit simultaneously large MO Kerr rotation and strong MCA and thus one can expect a large anisotropy of MO response from these compounds. However, the MOA in the MLS has not been observed so far as the above mentioned method of the experimental investigation of the MOA is inapplicable in this case because there exist only one probed surface, i.e. the film plane. The only way to study the MOA in MLS is to measure both the polar (where sample magnetization lies perpendicular to the sample plane) and longitudinal Kerr effect (LKE) (where sample magnetization lies in the plane of the sample and also in the plane of incidence of the light). This approach is more complicated as additional data on the optical constants are required to extract the off-diagonal optical conductivity. Besides, the amplitude of the LKE signal is much smaller than that of the PKE and a very sensitive registration method is required.

The present work provides the first direct experimental

* Corresponding author. Fax: +48-85-745-7223.
E-mail address: ubaluba@venus.uwb.edu.pl (L. Uba).

PII: S0038-1098(00)00080-6

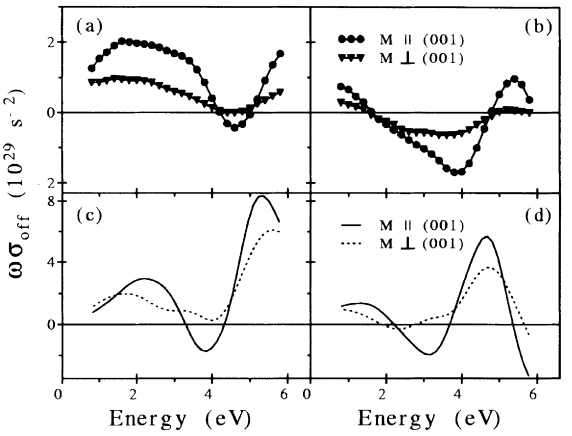

Fig. 1. Experimental absorptive (a) and dispersive (b) parts of the off-diagonal optical conductivity of Fe/Au MLS compared with the theoretically calculated ((c) and (d)) off-diagonal conductivity for Fe_1/Au_1 MLS.

observation of the MOA in MLS. The giant MOA as high as 200% has been observed in Fe(001)/Au(001) MLS and its origin quantitatively explained by the first-principles band-structure calculations. These calculations correctly describe the amplitude and the shape of the MOA spectra, identify the contributions coming from different interband transitions and demonstrate a very strong sensitivity of the MOA to the actual atomic structure at the interfaces.

The Fe/Au structures were chosen for the present study as they were investigated experimentally [12–14] and theoretically [15–17] and they demonstrate a unique combination of a high magnetic moment with a high Curie temperature and a high perpendicular anisotropy. These properties are connected with the formation of the $L1_0$ ordered structure, which does not exist in the Fe–Au phase diagram near equiatomic composition, but can be fabricated layer-by-layer by molecular beam epitaxy (MBE) [12,13,18,19]. Experimentally derived order parameter [12,13] was much lower than it could be expected from the layer-by-layer growth observed for the Au(001)/Fe(001) system [20]. Recently, the deterioration of the ordered $L1_0$ structure in the monoatomic Fe(001)/Au(001) MLS was explained by the conversion electron Mossbauer spectroscopy (CEMS) [18,19], involving the Au self-surfactant effect [20,21]. The vertical mass transport accompanying the multilayer growth leads to Fe aggregation, so that the resulting structure may be regarded as a mixture of a monolayer and double-layer (and to a less extent also the tri-layer) MLS.

2. Results and discussion

For the present studies, the well-characterized epitaxial $(Fe_1/Au_1)\times 20$ MLS, investigated previously by CEMS [18,19], was used. The sample was grown by the MBE in UHV conditions (base pressure during preparation below 5×10^{-10} mbar) on a 30 nm (001)Au buffer layer (preceded by a 4 nm Fe(001) seed layer), deposited on a MgO(001) cleaved substrates in a multi-stage process [20]. The whole structure was finally covered by a 5 nm Au cap-layer. The Fe and Au monolayers were deposited alternately at 340 K at the rate of about 0.2 mn/min, as controlled by a quartz microbalance with an accuracy of ±5%. The sample growth was monitored in situ by LEED, which documented epitaxial growth with the (001) orientation across the whole sample. The MO Kerr rotation and ellipticity spectra were measured at room temperature under saturation condition in the photon energy range of 0.8–5.8 eV at 2 and 75° incidence in PKE and LKE geometry, respectively, using a polarization modulation method [22,23]. The optical properties were measured directly by spectroscopic ellipsometry with the use of the rotating analyzer method. The correctness of the experimental procedure was checked by performing the measurements for the cubic YIG crystal and no spurious MOA was observed in this isotropic case. To extract the off-diagonal tensor components of the MLS from the measured effective optical and MO spectra, the multireflection calculations based on the Zak et al. formalism [24] were applied. The input data used for the MLS underlying layers were measured on the MgO(001)/4 nm Fe/30 nm Au control sample.

To provide a theoretical description of the observed MOA, we carried out ab initio band structure calculations for model Fe_1/Au_1 and Fe_2/Au_2 MLS. Fe_1/Au_1 is of $L1_0$ type structure [12,13]. In-plane lattice parameter ($a = 4.066$ Å) was taken so that the interatomic distances were equal to the average between bulk Au and Fe values. Interplanar spacing for Fe_1/Au_1 MLS was taken from the experiment [25] ($c/a = 0.960$). For the Fe_2/Au_2 MLS, we chose the interplanar spacing which minimize the total energy ($c/a = 1.889$). As the details of the computational method are described in our previous paper [22] we mention only some aspects here. The electronic structure of the compounds was calculated self-consistently using the local spin density approximation (LSDA) [26] and the fully relativistic spin-polarized LMTO method [27–30]. The **k**- space integrations were performed with the improved tetrahedron method [31].

Magneto-optical effects are determined by the off-diagonal components of the dielectric tensor of the material, whose amplitude is roughly proportional to the product of magnetization and SO coupling strength. Fig. 1 shows the experimentally obtained off-diagonal optical conductivity spectra in the MLS of nominal Fe_1/Au_1 structure for two orientations of magnetization: $M \parallel (001)$ ($\sigma_{\mathrm{off}}^{\parallel}$ for PKE), and $M \perp (001)$ ($\sigma_{\mathrm{off}}^{\perp}$ for LKE), together with the corresponding spectra calculated for the ideal Fe_1/Au_1 $L1_0$ structure. Considering as in Ref. [10] the ratio $(\sigma_{\mathrm{off}}^{\parallel} - \sigma_{\mathrm{off}}^{\perp})/\frac{1}{2}(\sigma_{\mathrm{off}}^{\parallel} + \sigma_{\mathrm{off}}^{\perp})$, we found that the measured anisotropy reached 200% at the photon energy 4.7 eV corresponding to the minimum of $\sigma_{\mathrm{off}}^{\parallel}$. The spectral dependence and the large value of the MO anisotropy were confirmed by the

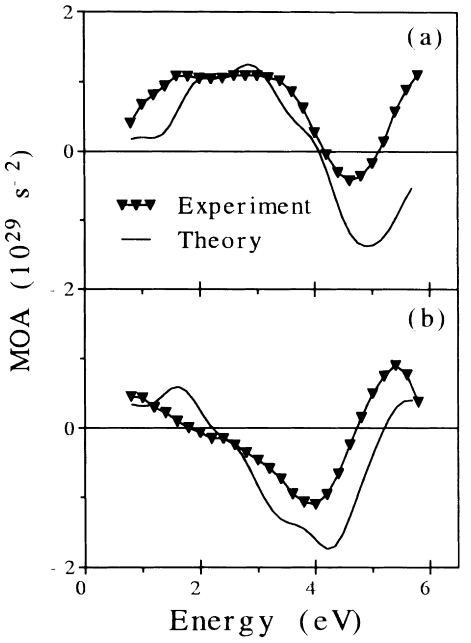

Fig. 2. (a) Experimental absorptive; and (b) dispersive part of the MOA of Fe/Au MLS in comparison with the theory (see text).

measurements performed for several other films of the nominal Fe_1/Au_1 structure. Overall, the experimental features are reasonably well reproduced in the LSDA calculations both in the spectral shape and the magnitude of the anisotropy. However, the position of the calculated prominent peaks at 3.8 and 5.2 eV is shifted towards smaller energies as compared to the experiment. One of the possible

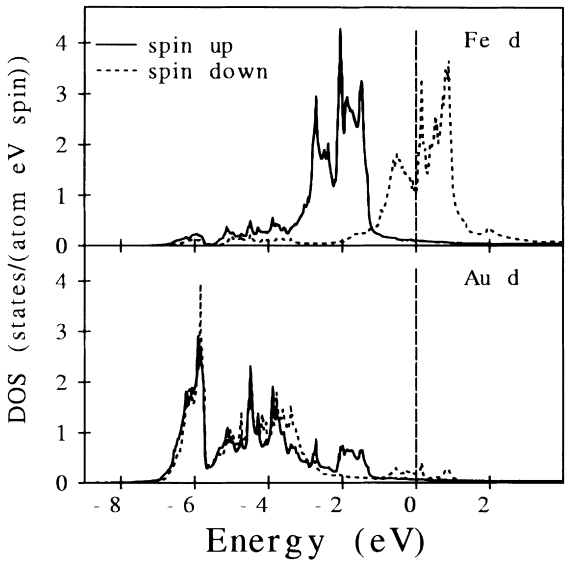

Fig. 3. LSDA spin-projected fully relativistic partial DOS (in states/(atom eV spin)) of the $L1_0$ ordered Fe_1Au_1 MLS.

Table 1
Calculated spin M_S and orbital M_L magnetic moments (in μ_B) of Fe_1/Au_1 versus magnetization direction

Atom	State	$M \parallel [001]$		$M \perp [001]$	
		M_S	M_L	M_S	M_L
Fe	d	2.894	0.099	2.895	0.063
Total		2.903	0.098	2.905	0.062
Au	d	0.103	0.028	0.105	0.029
Total		0.024	0.030	0.026	0.034

reasons is that due to the non-exact treatment of the electron exchange and correlation the LSDA underestimates the binding energy of d states and the threshold of interband transitions in noble metals compared to photoemission and optical measurements [32,33].

Even more important source of the discrepancies is that the studied structure is not ideal monoatomic Fe_1/Au_1 MLS but rather a mixture of mono- and double-layer structures. Having this in mind we modeled the effective optical conductivity of the structure by a weighted average of the conductivities calculated for the Fe_1/Au_1 and Fe_2/Au_2 MLS: $\sigma_{off} = x\sigma_{off}^{1/1} + (1-x)\sigma_{off}^{2/2}$. The best agreement between the theory and the experiment, both in the MOA (presented as $\omega\sigma_{off}^{\parallel} - \omega\sigma_{off}^{\perp}$ in Fig. 2) and the shape of the off-diagonal optical conductivity (not shown) is achieved with $x = 0.3$. This value agrees well with the results of the CEMS analysis which estimate the contribution of Fe_1/Au_1 MLS in the structure studied to be 32% [18,19]. As an opposite case to the structure with well defined mono- and double-layers, we examined also the effect of a possible alloying at the interfaces by calculating the MO spectra for MLS composed of Fe and Au monolayers separated by a single layer of Fe_1Au_1 ordered planar alloy. We found that the MO anisotropy is considerably reduced in this case. This clearly demonstrates the importance of actual atomic structure in the interface region for the determination of the MO spectra in the MLS and the ability of the MO spectroscopy to probe the microstructure on the monoatomic scale.

To understand the microscopic origin of the MOA better, let us consider in detail the electronic structure of the Fe_1/Au_1 $L1_0$ MLS. Spin-projected densities of Fe and Au d states are shown in Fig. 3 and the calculated spin and orbital magnetic moments are summarized in Table 1. Due to the smaller number of nearest neighbors of the same type, both Fe and Au d states are much narrower than in corresponding bulk metals. As a result, the majority spin Fe d states are fully occupied which leads to a significant enhancement of Fe spin magnetic moment (2.90 μ_B) compared to the value of 2.2 μ_B for bulk Fe. This enhanced magnetization has been observed [25] but the experimental value of 2.75 ± 0.25 μ_B is somewhat smaller than the calculated one.

Comparing the values of the magnetic moments calculated for different magnetization directions one can see

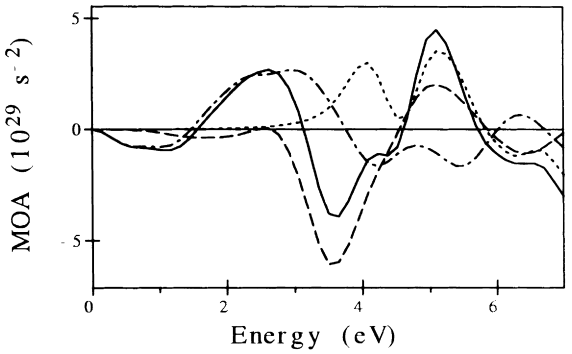

Fig. 4. Decomposition of the theoretically calculated MOA (solid line) into contributions coming from interband transitions from initial states of Fe $d_\uparrow$ (dashed line), Fe $d_\downarrow$ (dash-dotted line), and Au d character (dotted line).

from Table 1 that Fe spin moments are almost independent of the magnetization direction. At the same time the anisotropy of Fe orbital moment, which is determined mainly by Fe d states, is quite large and is of the same order of magnitude as it was experimentally observed in Co/Au MLS [34]. This behavior could be expected as in the presence of SO coupling the anisotropy of the orbital moment is of the order of ξ/Δ, where ξ is a SO parameter and Δ is crystal field splitting, while the anisotropy of the spin moment is proportional to $(\xi/\Delta)^2$ [35]. As Au d states are fully occupied, the spin and orbital moments at Au site are small and depend weakly on the magnetization direction. The total energy calculations show that the energy of the MCA $\Delta E_{\mathrm{MC}} \equiv E_{\mathrm{tot}}^{\parallel} - E_{\mathrm{tot}}^{\perp}$ in Fe_1/Au_1 is equal to -0.55 meV per formula unit and the easy magnetization axis is perpendicular to the surface in agreement with the experimental data of Ref. [12,13].

It is well known that the MO effects and the orbital magnetic moment are both caused by the SO coupling. However, the dependence of the MOA on the SO coupling and hybridization strengths is very complicated (see, e.g. Ref. [36]) and does not allow to introduce a simple model consideration as in the case of the MC anisotropy [2,3]. So, the only way to obtain a realistic description of the MOA is to perform numerical calculations. We examined the dependence of the MOA on the exchange splitting and the SO interaction as it is described in Ref. [37]. We found that the SO coupling of Au is equally responsible for the large MOA as the exchange splitting of Fe.

The optical conductivity can be expressed as a sum of additive contributions coming from interband transitions with the initial and/or final states lying in different nonoverlapping energy intervals. In the case of Fe_1Au_1, where Fe $d_\uparrow$, Fe $d_\downarrow$, and Au d states are rather well separated in energy (see Fig. 3), one can analyze the MO response itself and the MOA in terms of three contributions from transitions from initial states derived mainly from Fe $d_\downarrow$ ($-1.0 < E^{(i)} \leq E_{\mathrm{F}}$), Fe $d_\uparrow$ ($-3.5 < E^{(i)} \leq -1.0$ eV), and Au d ($E^{(i)} \leq -3.5$ eV) states (Fig. 4). From such an analysis it follows that in the photon energy ranges below ≈ 2.5 eV and above ≈ 4.5 eV the MOA is mostly determined by transitions from Fe $d_\downarrow$ and Au d states, respectively. Whereas the peak at ≈ 3.5 eV is mainly due to the interband transitions from Fe $d_\uparrow$ states.

We also calculated the energy band structure and MO spectra varying the c/a ratio in the Fe_1/Au_1 MLS. We found that both the MCA and the anisotropy of the orbital moment ΔM_{L} increase with an increase of c/a providing almost linear dependence of the MCA on ΔM_{L}, in a good agreement with the results of the perturbative approach [2,3] which show that for uniaxial systems in the case when the majority spin band is completely filled the energy of MCA is proportional to the anisotropy of the orbital moment. On the other hand, the dependence of the MOA on c/a is more complicated and depends strongly on the structure of a particular MLS. In Fe_1/Au_1 MLS, the MOA is almost independent of c/a in the energy range below 3.5 eV which corresponds to the interband transitions from mostly Fe $d_\uparrow$ states and decreases with an increase of c/a in the energy range above 3.5 eV where the transitions from Au d states dominate.

In conclusion, we have observed for the first time a giant MOA in Fe/Au MLS. The ab initio theoretical calculations describe well the measured spectra. The magnitude of the MOA is very sensitive to the actual atomic structure. It reduces as the number of adjacent layers of the same type increases, and almost disappears in the case of alloying at the interface. The interplay of the strong SO interaction on Au sites and the large exchange splitting on Fe sites through Au d–Fe d hybridization is responsible for the giant MOA, the strong anisotropy of Fe d orbital moments, and MCA.

Acknowledgements

This work is supported by the Polish State Committee for Scientific Research (KBN) under contract No. 2 P03B 113 11.

References

[1] For a review on magnetic multilayers, see J.A.C. Bland, B. Heinrich (Eds.), Ultrathin Magnetic Structures, Vols. I and II, Springer, Berlin, 1994.
[2] P. Bruno, Phys. Rev. B 39 (1989) 865 (and references therein).
[3] G. van der Laan, J. Phys.: Condens. Matter 10 (1998) 3239.
[4] J. Trygg, B. Johansson, O. Eriksson, J.M. Wills, Phys. Rev. Lett. 75 (1995) 2871.
[5] S.V. Halilov, A.Ya. Perlov, P.M. Oppeneer, A.N. Yaresko, V.N. Antonov, Phys. Rev. B 57 (1998) 9557 (and references therein).
[6] P.M. Oppeneer, V.N. Antonov, in: H. Ebert, G. Schütz (Eds.),

Spin–Orbit Influenced Spectroscopies of Magnetic Solids, Springer, Berlin, 1996, p. 29.
[7] S. Uba, A.N. Yaresko, L. Uba, A.Ya. Perlov, V.N. Antonov, R. Gontarz, H. Ebert, Phys. Rev. B 57 (1998) 1534.
[8] Yu.A. Uspenskii, E.T. Kulatov, S.V. Halivov, Phys. Rev. B 54 (1996) 474.
[9] E.A. Ganshina, G.S. Krinchik, L.S. Mironova, A.S. Tablin, Sov. Phys. JETP 78 (1980) 733.
[10] D. Weller, G.R. Harp, R.F.C. Farrow, A. Cebollada, J. Sticht, Phys. Rev. Lett. 72 (1994) 2097.
[11] R.M. Osgood III, K.T. Riggs, A.E. Johnson, J.E. Mattson, C.H. Sowers, S.D. Bader, Phys. Rev. B 56 (1997) 2627.
[12] K. Takanashi, S. Mitani, M. Sano, H. Fujimori, H. Nakajima, A. Osawa, Appl. Phys. Lett. 67 (1995) 1016.
[13] S. Mitani, K. Takanashi, H. Nakajima, K. Sato, R. Schreiber, P. Grünberg, H. Fujimori, J. Magn. Magn. Mater. 156 (1996) 7.
[14] S. Riedling, N. Knorr, C. Mathieu, J. Jorzick, S.O. Demokritov, B. Hillebrands, R. Schreiber, P. Grünberg, J. Magn. Magn. Mater. 198-199 (1999) 348.
[15] H. Miyazawa, T. Oguchi, J. Phys. Soc. Jpn 68 (1999) 1412.
[16] J.-T. Wang, Z.-Q. Li, Q. Sun, Y. Kawazoe, J. Magn. Magn. Mater. 183 (1998) 42.
[17] Z.-P. Shi, J.F. Cooke, Z. Zhang, M.M. Klein, Phys. Rev. B 54 (1996) 3030.
[18] T. Ślęzak, W. Karaś, M. Kubik, M. Mohsen, M. Przybylski, N. Spiridis, J. Korecki, Hyperfine Inter. 3 (1998) 409.
[19] J. Korecki, M. Kubik, N. Spiridis, T. Ślęzak, Acta Phys. Pol. 97 (2000) 129.
[20] N. Spiridis, J. Korecki, Appl. Surf. Sci. 141 (1999) 313.
[21] V. Blum, Ch. Rath, S. Müller, L. Hammer, K. Heinz, J.M. Garcia, J.E. Ortega, J.E. Prieto, O.S. Hernan, J.M. Gallego, A.L. Vasquez de Parga, R. Miranda, Phys. Rev. B 59 (1999) 15966.
[22] S. Uba, L. Uba, A.N. Yaresko, A.Ya. Perlov, V.N. Antonov, R. Gontarz, Phys. Rev. B 53 (1996) 6526.
[23] A.N. Yaresko, L. Uba, S. Uba, A.Ya. Perlov, R. Gontarz, V.N. Antonov, Phys. Rev. B 58 (1998) 7648.
[24] J. Zak, E.R. Moog, C. Liu, S.D. Bader, Phys. Rev. B 43 (1991) 6423.
[25] K. Takanashi, S. Mitani, K. Himi, H. Fujimori, Appl. Phys. Lett. 72 (1998) 737.
[26] U. von Barth, L.A. Hedin, J. Phys. C 5 (1972) 1629.
[27] O.K. Andersen, Phys. Rev. B 12 (1975) 3060.
[28] V.V. Nemoshkalenko, A.E. Krasovskii, V.N. Antonov, Vl.N. Antonov, U. Fleck, H. Wonn, P. Ziesche, Phys. Status Solidi B 120 (1983) 283.
[29] V.N. Antonov, A.Ya. Perlov, A.P. Shpak, A.N. Yaresko, J. Magn. Magn. Mater. 146 (1995) 205.
[30] V.V. Nemoshkalenko, V.N. Antonov, Computational Methods in Solid State Physics, Gordon and Breach, London, 1998.
[31] P.E. Blöchl, O. Jepsen, O.K. Andersen, Phys. Rev. B 49 (1994) 16223.
[32] K.A. Mills, R.F. Davis, S.D. Kevan, G. Thornton, D.A. Shirley, Phys. Rev. B 22 (1980) 581.
[33] E.E. Krasovskii, A.N. Yaresko, V.N. Antonov, J. Electron Spectrosc. 68 (1994) 157.
[34] D. Weller, J. Stöhr, R. Nakajima, A. Carl, M.G. Samant, C. Chappert, R. Megy, P. Beauvillain, P. Veillet, G. Held, Phys. Rev. Lett. 75 (1995) 3752.
[35] J. Stöhr, H. König, Phys. Rev. Lett. 75 (1995) 3748.
[36] H.S. Bennet, E.A. Stern, Phys. Rev. 137 (1965) A448.
[37] P.M. Oppeneer, V.N. Antonov, T. Kraft, H. Eschrig, A.N. Yaresko, A.Ya. Perlov, J. Phys: Condens. Matter 8 (1996) 5769.